Optimising ice flow law parameters using borehole deformation measurements and numerical modelling

Chandler, David M.; Hubbard, Bryn; Hubbard, Alun L.; Murray, Tavi; Rippin, David

Published in:
Geophysical Research Letters

DOI:
10.1029/2008GL033801

Publication date:
2008

Citation for published version (APA):
Chandler, D. M., Hubbard, B., Hubbard, A. L., Murray, T., & Rippin, D. (2008). Optimising ice flow law parameters using borehole deformation measurements and numerical modelling. *Geophysical Research Letters*, *35*(12). https://doi.org/10.1029/2008GL033801

Optimising ice flow law parameters using borehole deformation measurements and numerical modelling

David Chandler,[1] Bryn Hubbard,[1] Alun Hubbard,[1] Tavi Murray,[2] and David Rippin[3]

Received 28 February 2008; revised 3 April 2008; accepted 16 April 2008; published 19 June 2008.

[1] Internal ice strain rates have been measured along two boreholes drilled through Glacier de Tsanfleuron, Switzerland. Differences between these measurements and the output from a 3D numerical model of glacier motion have been minimized by a scheme that optimizes three rheological parameters in the constitutive equation for ice creep: the stress exponent n, the rate factor A, and a Lower Zone (basal ice) enhancement factor E_{LZ}. Results suggest that a linear rheology dominated by diffusion creep ($n = 1$) is more appropriate for modelling ice flow in this relatively thin (generally <80 m thick) glacier than the conventional $n = 3$, and that E_{LZ} is ~2. For $n = 1$, the predicted ice crystal size and value of E_{LZ} are both consistent with measurements made on ice cores recovered from the glacier, providing independent support for the optimization technique and the linear creep model. **Citation:** Chandler, D., B. Hubbard, A. Hubbard, T. Murray, and D. Rippin (2008), Optimising ice flow law parameters using borehole deformation measurements and numerical modelling, *Geophys. Res. Lett.*, *35*, L12502, doi:10.1029/2008GL033801.

1. Introduction

[2] Any ice flow model designed to investigate past or present glacier or ice sheet evolution requires well constrained ice rheology so that flow rates can be accurately predicted. At present it is widely assumed that strain rates in isotropic ice follow a power-law dependence on stress, with a flow law of the form

$$\dot{\varepsilon}_{ij} = A_0 E \exp\left(-\frac{Q}{RT}\right) I_{II}^{n-1} \tau_{ij} \quad (1)$$

where $\dot{\varepsilon}_{ij}$ and τ_{ij} are components ij of the strain rate and deviatoric stress tensors (respectively), A_0 is the rate factor, n is the flow law exponent, I_{II} is the second invariant of the deviatoric stress tensor, Q is the activation energy for creep, R is the universal gas constant, T is the ice temperature and E is a dimensionless strain rate enhancement factor determined by the bulk properties of the ice, principally reflecting liquid water and impurities within the ice and a preferred crystal fabric [e.g., *Marshall*, 2005; *Paterson*, 1994]. The main controls on E are crystal orientation anisotropy (if anisotropy is parameterised rather than being represented fully as a tensor), and the volume fraction of liquid water present either in inclusions or in the intergranular vein network.

[3] The parameters n, Q and A_0 are subject to considerable uncertainty [see *Goldsby and Kohlstedt*, 2001 for a detailed review] and each can vary according to the creep processes, effective stress, crystal size and fabric, impurity content, and liquid water fraction. A value of $n = 3$ is used in most glacier models but there is increasing evidence for a value of $n = 1$ at low deviatoric stresses [e.g., *Marshall et al.*, 2002; *Pettit and Waddington*, 2003]. E is also uncertain and is often either ignored (i.e., $E = 1$), or increased in a stepwise manner in the basal ice layer [*Hubbard et al.*, 2003; *Thorsteinsson et al.*, 1999].

[4] The aim of this paper is to report a new scheme for optimizing flow-law parameters in glaciers and to apply the scheme to Glacier de Tsanfleuron, Switzerland.

2. Field Measurements

[5] Glacier de Tsanfleuron is ~3 km long, has a surface area of ~3.2 km^2, and extends from ~2960 to 2480 m a.s.l.. Extensive ice radar surveys at 10, 20 and 50 MHz indicate that the maximum thickness of the glacier is ~135 m, and that over ~70% of the glacier area is less than 80 m thick. The glacier rests on limestone which drains meltwater away from the glacier bed into the subterranean karst system. The physical character of the glacial ice has been studied in detail both in the field and on ice cores extracted from the glacier. These studies [e.g., *Hubbard et al.*, 2003; *Tison and Hubbard*, 2000] indicate the presence of three distinct ice layers: a debris-rich basal layer of ~1 m thickness, termed the Basal Zone; an overlying basal layer composed of debris-poor, clear-facies basal ice ~10 m thick (the 'Lower Zone', LZ); and an Upper Zone (UZ) comprising the rest of the glacier consisting of bubble-foliated and debris-poor englacial ice.

[6] In contrast to most glaciers in similar settings, surface ice velocities measured at Glacier de Tsanfleuron show no significant seasonal variation, interpreted by *Chandler* [2005] as reflecting a failure to develop a channelized subglacial drainage system at the glacier during the summer. This uniformity probably reflects the loss of most excess summer meltwater into the underlying karst. However, the absence of a seasonal velocity signal is an advantage for the present study since annual averages of ice deformation and displacement can be used without the undesirable nonlinear effects of transient velocity increases. Measured surface velocities at the glacier (Figure 1) range from between 5 and 10 m yr^{-1} over its relatively shallowly-sloping middle reaches, to ~35 m yr^{-1} in deeper ice located towards the northern lateral margin of the glacier and on the glacier's relatively steep tongue. *Chandler et al.* [2006] concluded

[1]Institute of Geography and Earth Sciences, Aberystwyth University, Aberystwyth, UK.
[2]Department of Geography, Swansea University, Swansea, UK.
[3]Department of Geography, University of Hull, Hull, UK.

0094-8276/08/2008GL033801$05.00

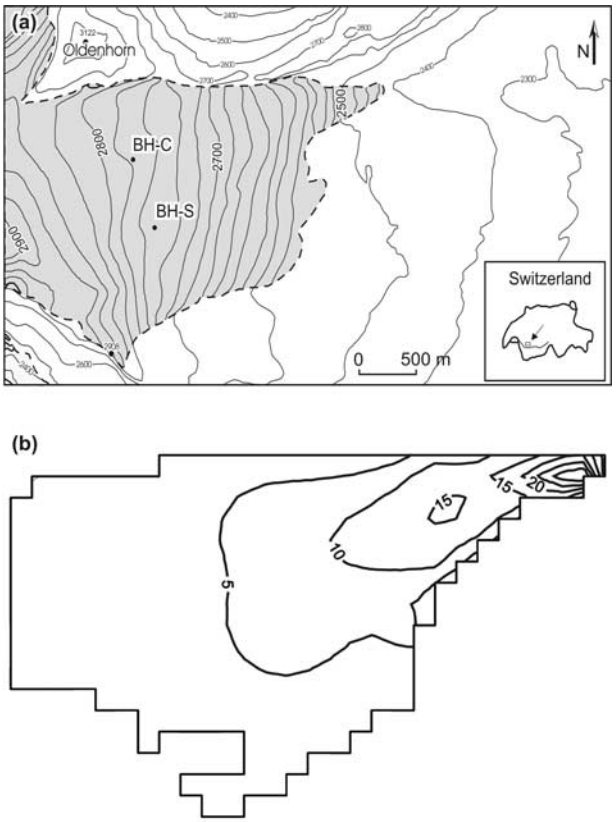

Figure 1. Glacier de Tsanfleuron: (a) basemap showing ice surface elevation and borehole locations ('BH-C' = central and 'BH-S' = south), and (b) the measured easterly component of surface velocity interpolated onto the 100 m grid used in the model. The northerly velocity component is everywhere less than 5 m yr^{-1}.

that a substantial fraction (between 45 and 84 %) of the glacier's surface motion was due to basal sliding.

[7] Internal strain rates were determined by repeat borehole inclinometry in two holes (Figure 1 and Table 1) drilled to the bed in 2004/05 (labelled south hole, *BH-S* and central hole, *BH-C*) and re-drilled in the summer of 2006. Borehole profiles were obtained using an Icefield Instruments MI-3 inclinometer, at 1 m intervals. In each survey, holes were inclinometered twice: once while the instrument was lowered, then again as the instrument was raised. The resulting profiles were averaged, leading to a maximum horizontal displacement error of approximately 3 mm per meter depth. Locations of borehole tops were measured by dGPS to an accuracy of ~0.1 m, and prisms used for velocity surveying were measured by optical survey to an accuracy of some millimeters [*Chandler*, 2005]. At-a-point sliding velocity was calculated by subtracting the local depth-integrated strain rate from the surface velocity.

3. Ice Flow Modelling and Parameter Optimisation

[8] Strain rates in the glacier are modelled using the three-dimensional finite-difference ice flow algorithms of *Blatter* [1995]. This is a first-order solution to the full Stokes equations and is valid for horizontal grid spacings greater than approximately one ice thickness. The vertical grid spacing is set to a constant fraction of the ice thickness, so that the glacier is split into *nz* discrete layers. Here, we use 60 layers and a horizontal grid spacing of 100 m. The latter exceeds the ice thickness at both boreholes and over 86% of the glacier's area. Borehole temperatures indicate that the glacier is predominantly temperate. We therefore assume the ice is isothermal and, with reference to equation (1) above, define the 'ice softness' $A = A_0 \exp(-Q/RT)$. With the assumption of isothermal ice, T and A are constant throughout the glacier.

[9] Since there is strong evidence for the existence of a distinct, softer Lower Zone in the basal ~10 m of the glacier [*Hubbard*, 2002; *Hubbard et al.*, 2003], the enhancement factor is specified as $E = E_{LZ} \geq 1$ for height $z \leq 10$ m and $E = 1$ for $z > 10$ m. Well constrained variables and parameters at Glacier de Tsanfleuron are as follows: the surface and bed topography from ice radar and dGPS measurements; the surface velocity [*Chandler*, 2005]; and the Lower Zone ice thickness [*Hubbard et al.*, 2003]. In addition, internal strain rates, and the ice surface and basal sliding velocities, are known at two locations from borehole measurements. Unknown quantities are the ice softness A, the Lower Zone enhancement factor (E_{LZ}), the flow-law exponent (n), and basal sliding velocities away from the two boreholes. Note that the 'sliding velocity' here includes both true ice-bedrock slip and any enhanced ice velocity within the thin but rheologically weak Basal Zone ice [e.g., *Hubbard*, 2002]). Such deformation could not be resolved with confidence from the inclinometer records, due both to the scale of the deformation (sub-meter) and its location (immediately above the ice-bed contact where hot-water drilling and basal drainage can widen the borehole base).

[10] The unknown sliding velocity is calculated in an iterative process of minimizing errors in the surface velocity field which has already been applied in 2D at this glacier [*Chandler et al.*, 2006]. Remaining unknowns are estimated by minimizing an error function that describes the match between the 3D measured and modelled strain rates. In the optimization scheme we use borehole strain rates rather than velocities, since measured velocities are subject to a downhole cumulative error. Errors in the measured strain rates are limited to the resolution of the inclinometer plus any local artefacts arising from the hole geometry. The latter error source can be reduced by using smoothed strain rates,

Table 1. Summary of Borehole Data[a]

Hole	Drilled	Re-drilled	H (m)	u_s (m yr^{-1})	v_s (m yr^{-1})	u_0 (m yr^{-1})	v_0 (m yr^{-1})
BHC	10/08/05	23/08/06	60	6.5	−0.5	5.8	0.6
BHS	09/04/04	10/08/06	57	4.0	−1.3	2.9	−1.2

[a]Shown are ice thickness H, surface velocity (u_s, v_s) and sliding velocity (u_0, v_0).

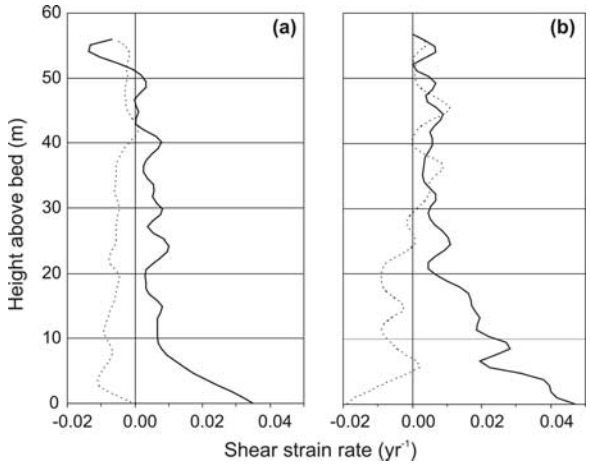

Figure 2. Measured shear strain rates $\dot{\varepsilon}_{xz}$ (solid lines) and $\dot{\varepsilon}_{yz}$ (dashed lines) in (a) the central borehole and (b) the south borehole.

obtained here using a five-point binomial smoothing function. The normalized *rms* error function ζ for strain rates is defined as

$$\zeta = \sqrt{\frac{\sum_{h,ij}\sum_{k=1}^{nz}\left(\dot{\varepsilon}_{ij,h,k}^{(MOD)} - \dot{\varepsilon}_{ij,h,k}^{(OBS)}\right)^2}{\sum_{h,ij}\sum_{k=1}^{nz}\left(\dot{\varepsilon}_{ij,h,k}^{(OBS)}\right)^2}} \quad (2)$$

The subscripts denote strain rate elements *ij* in layer *k* of hole *h*, and *nz* is the total number of layers. *MOD* and *OBS*, respectively, denote modelled and observed strain rates. Since there are two holes, each with two measured strain rate components $\dot{\varepsilon}_{xz}$ and $\dot{\varepsilon}_{yz}$), there are four individual (*h*, *ij*) components. Ice strain rates are greatest close to the bed, where they contribute most to ice transport, so we weight the error function linearly with depth to improve the match in this region. Equation (2) is then

$$\zeta = \sqrt{\frac{\sum_{h,ij}\sum_{k=1}^{nz}(nz-k)\left(\dot{\varepsilon}_{ij,h,k}^{(MOD)} - \dot{\varepsilon}_{ij,h,k}^{(OBS)}\right)^2}{\sum_{h,ij}\sum_{k=1}^{nz}(nz-k)\left(\dot{\varepsilon}_{ij,h,k}^{(OBS)}\right)^2}} \quad (3)$$

There are three key unknowns in the ice flow model: A, n and E_{LZ}. Therefore ζ is systematically calculated using a range of values for A, E_{LZ} and n, in the ranges $1 \times 10^{-16} \leq A_{UZ} \leq 3 \times 10^{-14}$ s^{-1} Pa^{-1} (with $n = 1$) or $1 \times 10^{-27} \leq A_{UZ} \leq 1 \times 10^{-24}$ (with $n = 3$); and $1 \leq E_{LZ} \leq 10$. For comparison, while $A = 6.8 \times 10^{-24}$ s^{-1} Pa^{-3} is the recommended rate factor for temperate ice with $n = 3$ [*Paterson*, 1994], initial tests showed this value resulted in strain rates and velocities that were considerably greater than those measured in the field. The two values for n were chosen explicitly to evaluate the relative performance of $n = 3$, as used in most previous modelling studies, and $n = 1$, which is gaining favour for ice at low deviatoric stresses, such as within the thin and shallow-sloping Glacier de Tsanfleuron.

4. Results

[11] Measured strain rates (Figure 2) are dominated by the longitudinal shear component ε_{xz} in both boreholes: most obviously in the lowermost 10 m in *BH-C* and 20 m in *BH-S*. With the exception of the basal ~5 m of *BH-S*, the transverse shear component ε_{yz} remains small along both boreholes (Figure 2). ε_{xz} is generally positive near the ice surface, and increases non-linearly with depth towards the bed. At both drill sites the ice motion is predominantly eastwards, consistent with both the surface geometry of the glacier (Figure 1) and previous velocities measured over a much wider area [*Chandler*, 2005]. Sliding contributes most of the total ice motion at both sites, accounting for 89% and 73% of the eastwards surface velocity at *BH-C* and *BH-S* respectively.

[12] Results of the optimization experiments (summarized in Table 2) generate error-function fields in the parameter space which converge consistently on single areas for both $n = 1$ (Figure 3a) and $n = 3$ (Figure 3b). This convergence on stable parameter combinations validates the experimental method and provides confidence in the results. In both fields the error function ζ reduces to below 0.6 within zones bounded by $1.5 < E_{LZ} < 3.5$, and contours away from these minima broadly following lines of constant AE_{LZ}. The main differences between the two experiment suites are that the minimum in ζ extends closer to $E_{LZ} = 1$ and the magnitude of ζ increases more rapidly for increasing E_{LZ} for $n = 1$ relative to $n = 3$.

Table 2. Empirical Data and Model Results for the Optimization Experiments[a]

				BH-C		*BH-S*	
n	A (Pa^{-1} s^{-n})	E_{LZ}	ζ	u_s (m yr^{-1})	u_b (m yr^{-1})	u_s (m yr^{-1})	u_b (m yr^{-1})
				Empirical			
–	–	1.8 – 3	–	6.5	5.8	4.0	2.9
				Model			
1	**2.5×10^{-15}**	**1.9**	**0.55**	**7.7**	**7.2**	**4.2**	**3.7**
1	4.1×10^{-15}	1.3	0.58	7.7	7.0	4.1	3.5
1	1.3×10^{-15}	3.0	0.59	7.8	7.4	4.2	3.9
3	**5.7×10^{-26}**	**2.5**	**0.59**	**8.0**	**7.5**	**4.4**	**4.0**
3	3.8×10^{-26}	3.5	0.60	8.1	7.5	4.5	4.0
3	1.3×10^{-25}	1.5	0.60	8.1	7.5	4.5	4.0

[a]First row: empirical data obtained using GPR, ice core analysis, dGPS and repeat inclinometry (described in text). Remaining rows: inversion results for model parameters n, A and E_{LZ}, along with their corresponding error function (ζ), and predicted surface velocity (u_s) and basal velocity (u_b). Parameter sets that minimise the error function are highlighted in bold.

[13] The best fit parameters for each suite of experiments are $A = 2.5 \times 10^{-15}$ s^{-1} Pa^{-1} and $E_{LZ} = 1.9$ ($\zeta = 0.55$) for $n = 1$, and $A = 5.7 \times 10^{-26}$ s^{-1} Pa^{-3} and $E_{LZ} = 2.5$ ($\zeta = 0.59$) for $n = 3$ (Table 2). Thus, the overall best fit is provided by the $n = 1$ model. However, the difference between the two fits is small ($\zeta = 0.04$) and the field defined by $\zeta < 0.6$ is fairly broad.

5. Discussion

[14] The large contribution from sliding suggested by both the field data and the optimization results is consistent with output from the 2D model applied at this glacier [*Chandler et al.*, 2006], where sliding was predicted to account for between 45% and 84% of the total surface velocity. Field evidence also indicates extensive sliding in the form of striations and carbonate crusts which occur over almost all of the exposed bedrock along the glacier's southern margin [e.g., *Hallet et al.*, 1978].

[15] Most ice sheet and glacier models have assumed a value of $n = 3$ on the basis of empirical evidence obtained in laboratory and field experiments [*Paterson*, 1994]. In this study, when $n = 3$ the best-fit values of A and E_{LZ} are 5.7×10^{-26} s^{-1} Pa^{-3} and 2.5 respectively (Table 2). This value for A is two orders of magnitude lower than that commonly used for temperate ice (6.8×10^{-24} s^{-1} Pa^{-3}; *Paterson* [1994]). However, the best-fit enhancement factor in the Lower Zone ($E_{LZ} = 2.5$) is close to that found by *Hubbard et al.* [2003], who calculated $E_{LZ} = 1.84$ from estimates of water content based on the chemical composition of the ice.

[16] A flow-law exponent of $n = 1$ implies ice deformation dominated by diffusion creep. This process has generally been neglected in glacier modelling, although it has been considered by, for example, *Pettit and Waddington* [2003] in investigating the dynamics of ice divides. Importantly, *Marshall et al.* [2002] also found evidence for $n = 1$ creep in a borehole deformation study on Worthington glacier, USA. Following *Goldsby and Kohlstedt* [2001], the rate factor for diffusion creep depends on the grain diameter d. Rearranging their equation (4) indicates that A decreases as d increases according to:

$$A = \frac{\varepsilon}{\sigma} = \frac{42 V_m}{RTd^2}\left(D_V + \frac{\pi\delta}{d} D_b\right) \quad (4)$$

Using the parameters estimated by *Goldsby and Kohlstedt* [2001] and assuming $T = 273$ K, the parameters in equation (4) are molar volume $V_m = 1.97 \times 10^{-5}$ m^3, volume diffusion and grain-boundary diffusion coefficients $D_V = 3.87 \times 10^{-15}$ m^2 s^{-1} and $D_b = 2.5 \times 10^{-13}$ m^2 s^{-1}, respectively, and grain boundary width $\delta = 5 \times 10^{-9}$ m. From equation (4), the best-fit value of A at Glacier de Tsanfleuron, as identified by our optimization scheme (i.e., $A = 2.5 \times 10^{-15}$ s^{-1} Pa^{-1}, Table 2), requires a grain size of $d = 0.8$ mm. This diameter is close to the values observed in unaltered englacial ice (typically 1–3 mm) measured in ice cores recovered from the glacier [*Tison and Hubbard*, 2000]. However, according to equation (4) the creep rate decreases as grain size increases, implying the grain size should be smaller in the softer Lower Zone.

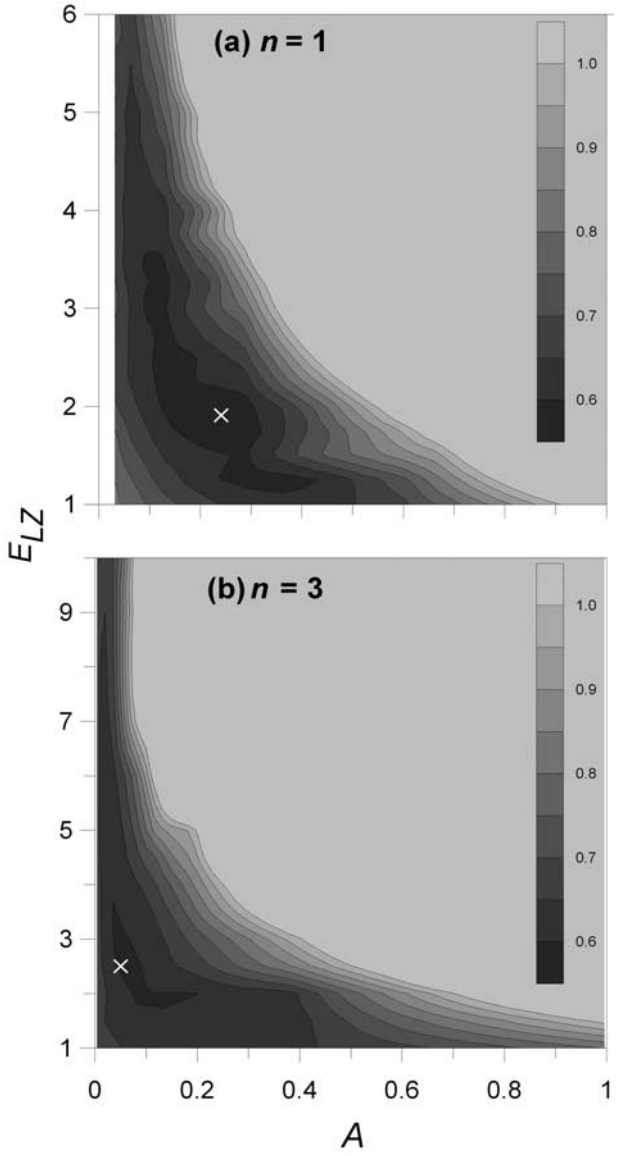

Figure 3. Error function ζ plotted as a function of E_{LZ} and A for optimization experiments with (a) $n = 1$ (in 10^{-14} S^{-1} Pa^{-1}) and (b) $n = 3$ (in 10^{-24} S^{-1} Pa^{-3}) calculated using the depth-weighted rms error given in equation (3). White crosses mark the error function minima. The generally hyperbolic shape of the minimization field reflects a trade-off between E_{LZ} and A, such that the greater the Lower Zone enhancement the less the ice mass as a whole needs to deform to attain the measured strain rates.

This contrasts with ice core measurements, which show a gradual increase in grain size with depth. This discrepancy might be explained by the increased liquid water content of the Lower Zone ice, estimated on the basis of ice radar to be ~3.9% [*Murray et al.*, 2007]. Inserting this value into *Duval*'s [1977] relation between ice softness and water content indicates that the basal layer will be ~3 times softer than the Upper Zone, englacial ice (i.e., $E_{LZ} \approx 3$ on the basis of radar-derived bulk ice water content). This enhancement is consistent with that yielded by the

optimization scheme above, providing further independent support for the scheme.

6. Summary and Conclusions

[17] Our optimization scheme, based on minimizing the difference between at-a-site modelled and measured 3D strain rate fields, successfully converges on stable parameter spaces when applied to Glacier de Tsanfleuron, indicating that the scheme is robust. Two optimization runs were carried out: one holding n constant at a value of 1, and the other holding n constant at a value of 3. The resulting best-fit values were provided by the $n = 1$ experiments, suggesting that the glacier may be considered to deform by diffusion creep. This case yields $A = 2.5 \times 10^{-15}$ s^{-1} Pa^{-1} and $E_{LZ} = 1.9$. Independent support for $n = 1$ is additionally provided by the close match between the crystal size predicted on the basis of diffusion creep and that measured at the glacier. The Lower Zone ice layer softens as a result of a high liquid water content, acquired by enhanced ice deformation as the glacier slides over its rough bed. Similar layers have been observed at numerous temperate glaciers, and independent ice radar and ice core analysis at Glacier de Tsanfleuron [*Hubbard et al.*, 2003] indicate its thickness is between ~10 and ~20 m. A soft basal layer such as this could therefore be applicable at any temperate glacier sliding over a rough substrate. The $n = 3$ optimization runs yielded a slightly poorer match and a particularly low value of A (5.7×10^{-26} s^{-1} Pa^{-3}).

[18] We therefore conclude that net ice flow in thin and/or shallow temperate glaciers such as Glacier de Tsanfleuron is best modelled using a flow-law exponent of $n = 1$ and including a 10–20 m thick basal ice layer that is twice as soft as the overlying englacial ice.

[19] **Acknowledgments.** This work was funded by UK NERC grant NER/A/S/2002/00607 and logistical support was provided by Gstaad 3000 AG. We thank two anonymous reviewers for their helpful comments.

References

Blatter, H. (1995), Velocity and stress-fields in grounded glaciers—A simple algorithm for including deviatoric stress gradients, *J. Glaciol.*, *41*, 333–344.

Chandler, D. M. (2005), Measuring and modelling glacier sliding, Ph.D. thesis, Univ. of Wales, Aberystwyth, U. K.

Chandler, D. M., A. L. Hubbard, B. Hubbard, and P. W. Nienow (2006), A Monte Carlo error analysis for basal sliding velocity calculations, *J. Geophys. Res.*, *111*, F04005, doi:10.1029/2006JF000476.

Duval, P. (1977), The role of water content on the creep rate of polycrystalline ice, *IAHS Publ.*, *118*, 29–33.

Goldsby, D. L., and D. L. Kohlstedt (2001), Superplastic deformation of ice: Experimental observations, *J. Geophys. Res.*, *106*, 11,017–11,030.

Hallet, B., R. Lorrain, and R. Souchez (1978), Composition of basal ice from a glacier sliding over limestones, *Geol. Soc. Am. Bull.*, *89*, 314–320.

Hubbard, B. (2002), Direct measurement of basal motion at a hard-bedded, temperate glacier: Glacier de Tsanfleuron, Switzerland, *J. Glaciol.*, *48*, 1–8.

Hubbard, B., A. Hubbard, H. M. Mader, J.-L. Tison, K. Grust, and P. W. Nienow (2003), Spatial variability in the water content and rheology of temperate glaciers: Glacier de Tsanfleuron, Switzerland, *Ann. Glaciol.*, *37*, 1–6.

Marshall, H. P., J. T. Harper, W. T. Pfeffer, and N. F. Humphrey (2002), Depth-varying constitutive properties observed in an isothermal glacier, *Geophys. Res. Lett.*, *29*(23), 2146, doi:10.1029/2002GL015412.

Marshall, S. J. (2005), Recent advances in understanding ice sheet dynamics, *Earth Planet. Sci. Lett.*, *240*, 191–204.

Murray, T., A. Booth, and D. M. Rippin (2007), Limitations of glacier ice-water content estimated using velocity analysis of surface ground-penetrating radar surveys, *J. Environ. Eng. Geophys.*, *12*, 87–99.

Paterson, W. S. B. (1994), *The Physics of Glaciers*, 3rd ed., 480 pp., Elsevier, New York.

Pettit, E. C., and E. D. Waddington (2003), Ice flow at low deviatoric stress, *J. Glaciol.*, *49*, 359–369.

Thorsteinsson, T., E. D. Waddington, K. C. Taylor, R. B. Alley, and D. D. Blankenship (1999), Strain-rate enhancement at Dye 3, Greenland, *J. Glaciol.*, *45*, 338–345.

Tison, J.-L., and B. Hubbard (2000), Ice crystallographic evolution at a temperate glacier: Glacier de Tsanfleuron, Switzerland, in *Deformation of Glacial Materials*, edited by A. J. Maltman, B. Hubbard, and M. J. Hambrey, *Geol. Soc. Spec. Publ.*, *176*, 23–38.

D. Chandler, A. Hubbard, and B. Hubbard, Institute of Geography and Earth Sciences, Aberystwyth University, Aberystwyth SY24 5JS, UK. (byh@aber.ac.uk)

T. Murray, Department of Geography, Swansea University, Singleton Park, Swansea SA2 8PP, UK.

D. Rippin, Department of Geography, University of Hull, Hull HU6 7RX, UK.